A New Remote Sensing Index for Assessing the Spatial Heterogeneity in Urban Eco-Environmental Quality Associated Road Network

Xincheng Zheng
Fujian Agriculture and Forest University
Zeyao Zou
Fujian Agriculture and Forest University
Chongmin Xu
Fujian Agriculture and Forest University
Sen Lin
Fujian Agriculture and Forest University
Zhilong Wu
Fujian Agriculture and Forest University
Rongzu Qiu
Fujian Agriculture and Forest University
Xisheng Hu (xshu@fafu.edu.cn)
Fujian Agriculture and Forest University
Jian Li
Fujian Agriculture and Forest University

Research Article

Keywords: Remote sensing based ecological index, geographically weighted regression, kernel density, road network, Fuzhou City

Posted Date: August 27th, 2021

DOI: https://doi.org/10.21203/rs.3.rs-845736/v1

Abstract

Although many prior efforts have found that road network has significantly affect the landscape fragmentation, the spatially heterogeneous effects of road network on the urban eco-environment remain poorly understood. To understanding the coupling mechanism of road network and eco-environment, a new remote sensing based ecological index (RSEI) was proposed to calculate the eco-environment quality, and kernel density of road (KDR) was applied to measure the road network density. We proposed a spatially explicit approach (geographically weighted regression, GWR) to explore the spatial variations in the relationship between the road network and the eco-environmental quality The results of GWR models fit better than those of the Ordinary Least Square (OLS) models. Among, the average effect of KDR on the variables of normalized difference vegetation index, land surface moisture and RSEI was negative, while it was positively associated with the variables of soil index, normalized differential build-up and bare soil index, index-based built-up index, and land surface temperature. From spatial perspective, the impacts of KDR on the urban boundary were generally greater than those on the city center. The spatial variation in the relationship between the road network and the eco-environment is mainly controlled by the relationship between the road network to the vegetation and the bare soil. Locally, the water body, whether a large regional river or urban inland rivers, has a great influence on the spatial variation in the relationship between the roads and the eco-environmental variables, and it can even change the sign of the influence.

Introduction

Roads appear as conspicuous objects in the world. Official statistics is staggering, with 4.8 million km^2 of highways in 2018 in China, 73,100 km^2 more than in 2017; 50.48 km/ 100 km^2 of highway density in 2018, increasing 0.76 km/ 100 km^2 from 2017. China's mountainous areas, including hills and plateaus, cover an area of 6.636 million km^2, accounting for 69.1% of the total land area in the country, which means these road networks might affect the eco-environment of a considerable part of the country’s earth surface. Previous studies suggest that roads might affect the eco-environment of nearly 15-20% of the total land area of the United States[1] and nearly 16% of the Netherlands[2]. Similarly, it has been reported that roads might impact proximately 20% of China’s land ecosystems[3]. It is projected that a further 25 million km^2 of road will be added on the earth by 2050 [4]. Such rapid extension of roads may impose serious eco-environmental threats and challenges in the future. Roads are clearly something worth understanding. To effectively avoid or mitigate the negative impacts of roads, it is essential to develop a systematic research framework to fully understand the road- impacts on eco-environment and their causal mechanisms[5]. Many of previous studies have focused on exploring landscape dynamics associated with road networks[6]. However, the landscape ecological effects on air, water, soil, and especially an integrated measure of eco-environment emanating from roads are not fully investigated[1,6,7]. Little knowledge on eco-environmental effects has been done in the heavily road sprawl zones in urban areas[8].

Roads have a wide array of ecological effects spreading through terrestrial and aquatic ecosystems[1]. First of all, road construction has huge ecological impacts early during the land use and cover changes[9], not only causing local habitat loss, but also increasing disturbances on surrounding landscapes[10]. Moreover, road extension may induce landscape fragmentation by cutting landscapes into pieces[6]. Specifically, great changes in landscape structure can be observed in most cased, as decreasing size of patches (core area size), increasing number of patches (patch density), and simplifying or complexing shape of patches (patch dimension)[11-13]. Reed et al.[14] quantified fragmentation caused by roads in southeastern Wyoming with several landscape structure measures, such as number of patches, mean patch area and perimeter-related indices so on, indicating that forest fragmentation was aggravated by cutting large plaques into smaller pieces and by transforming forest interior habitat into forest edge. Reed et al.[14] also pointed out that fragmentation could be reduced by minimizing or rerouting road construction. Karlson Mörtberg[15] explored potential effects of fragmentation and disturbance of roads on landscape in Swedish, revealing a main consequence of habitat loss of road effects. Meanwhile, the destructive effects of roads on wildlife have even been reported as one of the major crises of the global biodiversity[16].

From many perspectives, the detrimental impacts of roads on nature (both terrestrial and aquatic) ecosystems have been fully explored[5,15], however, eco-environmental impacts of road networks on urban area have gotten little attention[8]. Previous studies on the landscape effect of roads have emphasized on the spatial structure and pattern dynamics, while little analysis has been done in the eco-environmental function or quality for the urban area even with a dense road network. Wu et al.[17] also assessed the effects of a highway on landscape patterns in a town of Taiwan province. They discovered that the combination of highway construction and its subsequent urbanization had caused landscape isolation and fragmentation in the study area. Besides of the biological ecosystem, roads have a great impact on the abiotic ecosystem, such as air, water, and temperature as well[1]. For example, the direction of the road affects the ventilation of a city, which will affect the thermal field distribution of a city. Moreover, road motor vehicle is also one of the main sources of carbon emissions[5]. It has been reported that nearly 20% of the world's carbon dioxide (CO_2) emissions are generated from road traffic, the proportion is nearly 8% in China in 2015, and these emissions are increasing annually[7]. These may aggravate the deterioration of the urban eco-environment, such as the heat island effect. Severe health consequences for humans, coupled with a limited knowledge of how these landscape fragmentations caused by roads and road traffic pollutions jointly affect eco-environmental quality in urban area, highlight an urgent need to fill the knowledge gap of the couple relationship between roads and eco-environmental quality from a perspective of landscape. This will shed light on the mitigation measures for urban eco-environmental planning.

The need for sustainable planning and decision making for urban has stressed the construction of a framework to address effectively the eco-environmental quality. Among, Environmental Impact Assessment (EIA) and Strategic Environmental Assessment (SEA) are two legal frameworks to evaluate, project and mitigate adversely ecological effect of transport infrastructure; the Convention on Biological Diversity (CBD), the European Landscape Convention (ELC) and the EU Biodiversity Strategy (BS) also address the treatment of ecological impacts[10]. These analysis frameworks have been extensively employed in the studies of environmental assessment[18,19]. However, these frameworks emphasized the protection of habitat and the increasing of landscape connectivity for conserving biodiversity and ecosystem service. Moreover, these methods are only applicable to certain project or administrative division, while they are not feasible to explain the spatial distribution of ecological conditions and their changes for a region[20,21]. These problems are extremely important for propose an effective index to identify spatial variation in the eco-environmental impact of roads.

Recent advances in the availability of satellite-based datasets and remote sensing technology have provided a powerful tool to identify eco-environmental status at the pixel level with complete coverage for various ranges from local to global[22,23]. Therefore, remote sensing techniques have been extensively employed in eco-environmental observations on the earth[24,25]. A number of remote sensing indices, including a single factor (e.g., enhanced vegetation index, EVI; leaf area index, LAI; normalized difference vegetation index, NDVI; land surface temperature, LST) [26-28] and aggregated index (e.g., MODIS global disturbance index, MGDI; forest disturbance index, DI; scaled drought condition index, SDCI)[29-31]. More recently, Xu et al.[20] coined a remote sensing based ecological index (RSEI) by integrating four indicators, including greenness, wetness, dryness, and heat. The applications of RSEI suggest that it can effectively assess eco-environmental conditions in different regions[20-22,24].

Fuzhou City is in the southeast coast of China, which has experienced very rapid urbanization over the past three decades, with built-up area increasing more than 15 times from 22 km^2 in 1978 to 357 km^2 in 2018 [32]. Urban sprawl combining with the basin-like topography make it a new “stove” in China. Therefore, these features of the city make it a particular interesting case for exploring the spatial relationships between the roads and the eco-environmental quality. At present, the utility of remote sensing indicators as a tool to identify the impacts of roads in eco-environmental quality remains a challenge since their relationships may vary across the study area (i.e., spatial non-stationarity). To our knowledge, the spatial non-stationarity in the relationships between roads and eco-environmental quality has rarely been explored. Therefore, taking Fuzhou City as a case, we employed geographically weighted regression (GWR), a local model, to explore the spatial non-stationarity in the relationships between the kernel density of road (KDR) and RSEI across the study area. The following questions were explored: 1) Do the effects of roads on RSEI and its constituent factors vary with locations across the study area? 2) Does trade-off or synergy relationships between the two regressors predominate? 3) How do their relationships distribute? Results for the above

three questions will improve our knowledge on urban eco-environmental pattern and enhance improve our capability in road network and urban planning.

Materials And Methods

Study area. Fuzhou City is the capital and the largest prefecture-level city in the Fujian Province of China (Fig. 1), which is in the west coast of the Taiwan Strait and in the lower reaches of the Minjiang River. The average annual temperature is approximately 293.9 K. The annual precipitation varies widely from 796.5 to 1 913.6 mm, with approximately one-third receiving in the May and June. The study area (Fig. 1b) is the downtown area of the city, with dense buildings and population. It has been witnessed that the eco-environmental quality has been deteriorating dramatically in the past two decades[33]. And the city becomes one of the four new furnaces in China. Consequently, the study on spatial variations in the associations between the eco-environment quality and the road networks is very necessary, and may shed a light on those of rapidly urbanization region in the world.

Data resources and pre-processing. Landsat OLI/TIRS image used in this study was acquired on 2016-06-25. The road network dataset was obtained from OpenStreetMap. The pre-processing of the Landsat image includes radiometric calibration and atmospheric correction. For detailed steps, please refer to our published literature[22,24].

Calculation of remote sensing based ecological index. Remote sensing based ecological index (RSEI) is a synthetic index could assess a region's eco-environmental quality quickly and quantitatively, which was based on the pressure-state-response framework (PSR) using a principal components analysis (PCA)[22,24]. RSEI is capable of overcoming the weakness of most of the previous ecological indicators, which measure merely the response of the ecosystem to anthropogenic stresses causing impairment. The RSEI is composed of a couple of indicators, including the greenness, dryness, heat, and humidity, which were represented by normalized difference vegetation index (NDVI), normalized differential build-up and bare soil index (NDBSI), land surface temperature (LST) and land surface moisture (LSM), respectively. For NDBSI, which was calculated by combining soil index (SI) and index-based built-up index (IBI). All these indicators can be quickly obtained from Landsat datasets at the pixel level. The calculation formulas of these indicators and the synthesis of RSEI are detailed in the references[22,24].

Estimation of kernel density of road. The kernel function is used to calculate the road network density (i.e., KDR) per unit area based on points to fit each point to a smooth cone-shaped surface by moving windows[34]. The kernel function used was adapted from the fourth-order kernel function used to calculate the point density described in Silverman's book[35]. The search radius (bandwidth) of moving windows within which the density is calculated according to the "Silverman rule of thumb" spatial variable, which can effectively avoid spatial outliers (that is, points that are too far away from other points). The KDR map produced in the ArcGIS, in which the specific parameter design can refer to a previously published paper[36].

Sampling. Using ArcGIS software, a fishing net of 300·300 m was established as sampling unit, with a total of 7,796 samples for the study area (Fig. 2). The tool of Zonal Statistics as Table was employed to summarize the average values of all rasters within each sample of the datasets of each variable, and the statistics tables for all the variables were outputted. Then, all the average values in the output tables were joined to the sample layer based on the predetermined field. Thus, the sample layer had the attributes (i.e., the average value) of all variables at 300·300 m polygons, which can be used as input feature in modeling spatial relationships in ArcGIS.

Regression models. Both a global model (ordinary least squares, OLS) and a local model (GWR) were employed to examine the association between the RSEI associated indices (including NDVI, IBI, SI, NDBSI, LST, LSM, and RSEI) and KDR, respectively. The OLS models were used to detect the overall relationship between each two regressors, while the GWR models were applied to identify the spatial heterogeneity in the interactions between the two regressors across locations[32]. The regression models were simulated in the ArcGIS program. The KDR was set as independent variable, and NDVI, IBI, SI, NDBSI, LST, LSM, and RSEI were set as dependent variable in each separating model. In terms of the GWR models, the adaptive kernel type was set, and the bandwidth of the kernel was determined using the Akaike Information Criterion (AICc). The goodness of the models was evaluated using the following test indicators[32], including the adjusted R-squared, AICc, residual squares, P-value, and Moran's I.

Results

Tests of GWR and OLS models. Table 1 indicated the test results of the OLS and GWR models for fitting the associations between the KDR and the RSEI variables. The higher adjusted R^2, the smaller AICc values of the GWR models against the OLS models, indicate the goodness of the GWR models than the OLS ones. The relatively small in the values of Moran's *I* (0.199–0.309) reveals the small spatial autocorrelation in the Residual Squares (Figs. 3B,D,F,H,J,L,N), indicating the random distribution in the residuals across the study area. Moreover, all the seven GWR models were statistically significant at the 0.001 level, also indicating highly goodness fitting for all the GWR models. This supports the use of the GWR model in this study.

Summary of coefficients of the GWR models. Table 2 presents parameter descriptive statistics of the GWR models. These statistics can be used to compare the coefficient changes of different variables and reveal the variation of the coefficients in the study area. specifically, the impacts of KDR on all the RSEI indicators were both positive and negative across the study region. Except the variable of LST, whose values were not between − 1 and 1, the impacts of KDR on the other variables (from large to small) were in the order of NDVI, RSEI, SI, NDBSI, IBI and LSM. Among, the average effect of KDR on the variables of NDVI, LSM and RSEI was negative, while it was positive on the variables of IBI, SI, NDBSI, and LST.

Spatial variations in the response of RSEI indicators to KDR. GWR regression coefficients were mapped at grid level in Figs. 3A, C, E, G, I, K, M. In these maps, the Jenks method was employed to classify the coefficients into five categories, with zero being artificially set as a demarcation point to distinguish the positive and negative effects.

Figure 3A, B showed that the negative relationships between the KDR and the NDVI were distributed across most of the study area. This indicated that the NDVI increased gradually as the decreasing of the KDR, whereas the rates of decreasing varied significantly across the study region. The negative correlation coefficients were noticeably higher in the south part (i.e., the green clusters), while the negative correlation coefficients were obviously lower in the extensively northern areas (i.e., the brown clusters), where is the urban central area. However, a narrow stripe (2 km or so) located close to the river, exhibited a positive correlation between the KDR and the NDVI, indicating that the NDVI increased gradually as the increasing of the KDR.

Figure 3C, D indicated that the positive relationships between the KDR and the IBI were dominantly distributed in the study area, which indicates that the IBI increased gradually as the increase of the KDR. The figure also showed that the impact of the KDR on the IBI varied significantly across the region, with the positive correlation coefficients being noticeably higher in the boundary regions (i.e., the red clusters), while being obviously lower in the extensively central and northern areas (i.e., the yellow clusters). However, a narrow stripe (2 km or so) located close to the river, was observed to be negatively correlated with the IBI, indicating that the IBI decreased gradually as the increasing of the KDR.

Figure 3E, F revealed the spatial variations in the relationships between the KDR and the SI. The figure revealed that the positive correlations between KDR and SI occupied most of the study area. The positive correlation presented a basin-like trend, with low values in the middle and high value in the surrounding of the study area. Similar to the Fig. 3A, B, there was also a narrow stripe closer to the river, indicating noticeably negative associations between the KDR and the SI, indicating that the SI decreased gradually as the increasing of the KDR.

Figure 3G, H indicated the spatial variations in the relationships between the KDR and the NDBSI. The law of the spatial distribution was similar to that of the Fig. 3C, D. The figure showed that the positive correlation prevailed over the negative correlation in the study area. The positive correlation coefficients being noticeably higher in the boundary regions (i.e., the red, brown, and yellow clusters), while being obviously lower in the extensively central and northern areas (i.e., the green clusters). Moreover, there was a narrow stripe (2 km or so) located close to the river, being observed to be negatively correlated with the NDBSI.

Figure 3I, J also indicated a similar pattern in the relationships between the KDR and the LST, with those of the KDR and the IBI (Fig. 3C, D). In Fig. 3I, J, the warm colour (i.e., red, brown, and yellow) represented positive relationship, and the cool colour (i.e., green) indicated negative relationship. Similar to Fig. 3C, D, the positive correlation prevailed over the negative correlation in the study area. The positive correlation coefficients being noticeably higher in the boundary regions (i.e., the red, brown, and yellow

clusters), while being obviously lower in the extensively central and northern areas (i.e., the green clusters). Moreover, there was a narrow stripe (2 km or so) located close to the river, being observed to be negatively correlated with the LST.

Figure 3K, L revealed the spatial variations in the relationships between the KDR and the LSM. The relationships demonstrated that the negative relationship between the KDR and the LSM distributed in most of the study areas, indicating that the LSM decreased with the increase of the KDR. However, there were also quite a part of the study areas showing a positive relationship, distributing in the central area of the urban and the southern of the study area, where happened to be distributed in the negatively correlated places of the KDR and the IBI, and the KDR and the LST as well (Fig. 3C, D and I, J).

Figure 3M, N indicated the pattern of the relationships between the KDR and the RSEI, similar with those of the KDR and the NDVI (Fig. 3A, B), while opposite with those of the KDR and the SI (Fig. 3E, F). In Fig. 3M, N, the red cluster represented positive relationship, which was a narrow stripe (2 km or so) located close to the river, while the other areas were all in negative associations. Similar to Figs. 3A ,B and E, F, the negative/positive correlation coefficients were noticeably higher in the south part (i.e., the green/red clusters), while the negative/positive correlation coefficients were obviously lower in the extensively northern areas (i.e., the brown and yellow/light green clusters).

Correlation analysis between ecological indicators. To investigate the interactions between eco-environmental indicators, the Pearson correlation analysis and 2D-scatter plot were employed here. The sampling was implemented randomly using a 10·10 grid across the study area. It can be seen from the results of the Pearson correlation analysis (Table 3) that the SI and the RSEI values and their GWR regression coefficients have the greatest correlation among all the other pairs of variables, with the R^2 as high as -0.989; while the NDVI and the RSEI also have strong positive relationships. The scatter plots also show high linear relationships between them (Fig. 4). Due to the water and soil loss in the upstream of Minjiang River, there is a lot of sediment in the river body, leading to the distribution of SI index to be different from other indexes, with the differences of the SI values between the land surface and water body are much smaller than those of the other indexes. For example, the eco-environmental indicators, such as NDVI, IBI and NDBSI, all show a binary distribution pattern between the land surface and water body.

Discussion

From the regression results, the OLS models indicated statistically significant relationships between KDR and the RSEI composed indicators (R^2 = 0.013 ~ 0.168, p-value = 0.05), while the GWR model showed more considerably stronger relationships from the same datasets (R^2 = 0.314 ~ 0.564, p-value = 0.001), highlighting a tendency of spatial non-stationary in the relationships (Table 1). The main reason is that the conventional ordinary least squares regression models, assuming spatially stationary in the relationship between the regressors. Such assumption may often be untenable by ignoring the local variations of variables in each sample site, particularly in the large-scale studies based on remote sensing images[37–39]. Local statistical approaches (e.g., GWR), can be more appropriate than global techniques (e.g., OLS), if the relationship is spatially non-stationary[40]. GWR can capture the spatial variations in the relationship between variables, by including the spatial coordinates of the sample grids in the model. Therefore, GWR has huge potential in the studies using remote sensing data, as such data commonly have an explicit spatial character. However, the method is not a panacea, with essential issues, such as the calculation of weight matrix, in the processing of the model[38]. The weights are set to ensure the observations having more influence on nearer locations than those further away in the estimating of the parameters. The weights depend on a spatial kernel function in a bandwidth. Previous studies have often used a fixed bandwidth with a Gaussian function to assign sample plots for each regression and their spatial weights[41]. The assumption of a fixed bandwidth is that the sample plots are regular and consistent in size. An adaptive bandwidth is recommended in the uneven distribution of observations, in which the kernel bandwidth is based on the rule of the Akaike information criterion (AICc)[42]. This kind of bandwidth is adaptive in size to guarantee a same number of samples including in each regression[43]. In this study, we selected adaptive bandwidths with the Gaussian spatial kernel because of the uneven distribution of data, and used Moran's *I* index to examine spatial autocorrelation of the GWR residuals (Fig. 3). The goodness of fitting indicates effective of the local models and obviously superior to the conventional OLS models. We hope this study may again shed a new light on the potential regression or prediction analysis using remote sensing as a source data.

Upgrading and extending of road network has improve the accessibility of remote places, subsequently, triggering the sprawling of artificial landscape, as well as the human disturbances[44]. Road network has thus become a focus of interest in landscape ecology research. Many studies have focused on the relationship between the road network and landscape ecology in a range of spatial and temporal scales[6,45,46]. Thus, the quantification of the characteristics of road network and ecosystem is a priority in understanding the coupling mechanism. In terms of road network, road density is among the most commonly used index, which has been proved to be an effective indicator of road network, and associated with many eco-environmental effects[47]. However, the limitation of this classis indictor is that the value is the same in each entity, ignoring the spatial heterogeneity of road network distribution even in a homogeneous space[48]. Therefore, unlike many of studies that use road density indicator, we employ a more effective indicator (KDR) to measure road network at the pixel level[33,49]. In terms of ecological aspect, though different studies of road impact on landscape have been distinct in detail, each has inevitably measure landscape metrics (e.g., fragmentation, connectivity) for a region or an observation unit[33,50]. These landscape metrics are either patch level, landscape level, or moving window level[51], which are relatively coarse in terms of spatial resolution. In comparison with these landscape metrics, we employed a newly proposed remote sensing based ecological index (i.e., RSEI) at the pixel level to match the measurement of road network (i.e., KDR). RSEI has been coined by Xu et al.[52] and extensively applied to quantify and detect eco-environmental changes at various scales[21,32,52]. Our previous published papers have illustrated that this index can assess the regionally eco-environmental status objectively and easily[22,32]. These support our usage of the KDR and RSEI as proxy of road network and eco-environmental status, respectively, to explore the spatial variations in their relationships.

Since spatial non-stationarity may be common for most geographical events, local information should be included in regression analyses[53]. By identifying local variation in the relationships between the KDR and RSEI (including its sub-indicators) which may be missed using a global method, the GWR model was employed in this paper to act as a spatial microscope, revealing both synergy and trade-off locations, which is more feasible for future targeted measures. Our evidence revealed that the relationships were multiple, with different symbols of coefficients coexisting and varying across locations in the study area (Fig. 3). Thus, our outputs may provide a more scientific base for furtherly understanding of the mechanism how road network impacts on the observed RSEI values, and the variables of NDVI, IBI, SI, NDBSI, LST, LSM as well.

This was most apparent on the banks of the rivers, which contained a strip cluster showing an opposite relationship with KDR, compared with most of the study area, and the clusters varied across each variable (Fig. 3). This shows that the water body has a great influence on the relationship between roads and the eco-environment, and is the main influencing factor of the spatial variation of the relationship. Previous studies have revealed that the variations of the mapped coefficient values (Fig. 3) appear to connect with land cover patterns[32,38]. This is mainly because the spectral characteristics of water bodies are very different from those of other land use types, which is manifested by strong absorption in the near-infrared band, resulting in significant differences in the remote sensing retrieval index values of water bodies with other land types[54]. Moreover, due to the spill-over effect of high-density buildings in the urban center, the eco-environmental status of riversides is similar to that of urban centers[22], but these riversides land use patterns are usually different with those of the urban centers, with high coverage of green places, and low density of the road network. Therefore, the relationship between the road network and the eco-environment in the riverside is opposite to the other area of the urban. Specially, the narrow stipe (2 km or so) located close to the river, exhibiting a positive relationship between the KDR and the NDVI/RSEI, a negative relationship between the KDR and the SI, is due to the better greened road network and the less bare lands in such new district. The narrow stripe (2 km or so) located close to the river, with negative relationship between the KDR and the NDBSI/IBI, is due to the low construction density in such High-tech Development Zone. Moreover, the negative relationship between the KDR and the LST is because that there are more wetlands in the riverside, which has a cooling effect.

It should also be noted that all the impacts of road network on the RSEI and its indicators of urban boundaries (urban-rural junctions) were greater than that of urban centers, the southern part was among the most sensitive area with the highest values of all coefficients for all the eco-environmental variables (Fig. 3). This is because the density of road network in the urban center is relatively high and therefore has a high KDR value, while the urban-rural junction is the opposite. While the values of the eco-environmental indicators are relatively consistence ranging from − 1 to 1, the higher the KDR value, the lower the regression

coefficient is, otherwise the opposite. It is worth mentioning that the locally spatial variation in the relationships between the road network and eco-environmental indicators would have gone buried by a global regression analysis[42]. Moreover, the statistically significant relationships derived from the OLS models (Table 1), could lead to inappropriate and unproductive effort being directed towards discovering potential spatial variability in the relationships.

Conclusion

Both OLS and GWR models were employed to explore the spatial variations in the relationship between the road network (i.e., KDR) and the eco-environmental quality (i.e., RSEI), and the land surface parameters (i.e., NDVI, IBI, SI, NDBSI, LST, LSM) as well, with the Landsat-8 OLI/TIRS data in the megacities of Southeast China. The results show that the GWR models fit better than those of the OLS models, which supports our use of the GWR approach. Both positive and negative associations between the KDR and all the eco-environmental and land surface variables coexisted across the study area. Except the variable of LST, whose values were not between − 1 and 1, the impacts of KDR on the other variables (from large to small) were in the order of NDVI, RSEI, SI, NDBSI, IBI and LSM. Among, the average effect of KDR on the variables of NDVI, LSM and RSEI was negative, while it was positive on the variables of SI, NDBSI, IBI, and LST.

The spatial patterns of GWR coefficients indicated that (1) The impacts of KDR on the urban boundary were generally greater than those on the city center. (2) The response of urban eco-environment and land surface feature to road network was affected greatly by water area, whether a large regional river (i.e., the Minjiang River) or urban inland rivers. Rivers may change the sign of the relationships between the road network and the variables. Because the river itself and the riverside have special land cover features, such as covered by wetland parks and low-density buildings. (3) The spatial variation in the relationship between the road network and the eco-environment is mainly controlled by the relationship between the road network and the vegetation and the relationship between the road network and the bare soil.

Declarations

Author contributions

X.Z.: Writing-Original draft, Methodology, Formal analysis, Data curation, Software, Visualization, Z.Z.: Formal analysis, Data curation, Software, Visualization, C.X.: Formal analysis, Data curation, Software, Visualization, S.L.: Formal analysis, Data curation, Software, Z.W.: Formal analysis, Data curation, Software, R.Q.: Supervision, X.H.: Conceptualization, Validation, Writing- Review & Editing, Supervision, J.L.: Supervision.

Funding information

This research was funded by the China Postdoctoral Science Foundation (no. 2017M610390), the National Natural Science Foundation of China (no. 31971639), and the Natural Science Foundation of Fujian Province (no. 2019J01406), to which we are very grateful.

Competing interests

The authors declare no competing interests.

Data availability

All relevant data are included in the papers. Contact corresponding author for additional information regarding data access.

References

1. Forman, R.T.T., Sperling, D., Bissonette, J.A., Clevenger, A.P., Cutshall, C.D., *et al*. Road Ecology: Science and Solutions (ed. Island Press), (Washington, DC, 2003).

2. Reijnen, R., Foppen, R., Veenbaas, G. Disturbance by traffic of breedingbirds: Evaluation of the effect and considerations in planning and managingroad corridors. *BIODIVERS CONSERV.* **6**, 567-581 (1997).
3. Li, T., Shilling, F., Thorne, J., Li, F., Schott, H., Boynton, R., M, B.A. Fragmentation of China's landscape by roads and urban areas. *LANDSCAPE ECOL.* **25**, 839-853 (2010).
4. van der Ree R, J, S.D., C, G. Handbook of Road Ecology (ed. John Wiley & Sons) (Hoboken, NJ, 2015).
5. Leonard, R.J., Hochuli, D.F. Exhausting all avenues: why impacts of air pollution should be part of road ecology. *FRONT ECOL ENVIRON*. **15**, 1-7 (2017).
6. Hosseini, V.M., Salmanmahiny, A., Monavari, S.M., Kheirkhah Zarkesh, M.M. Cumulative effects of developed road network on woodland—a landscape approach. *ENVIRON MONIT ASSESS*. **186**, 7335-7347 (2014).
7. Zhang, L.L., Long, R.Y., Chen, H., Geng, J.C. A review of China's road traffic carbon emissions. *J CLEAN PROD*. **207**, 569-581 (2019).
8. Zhu, M., Xu, J.G., Jiang, N., Li, J.L., Fan, Y.M. Impacts of road corridors on urban landscape pattern: a gradient analysis with changing grain size in Shanghai, China. *LANDSCAPE ECOL*. **21**, 723-734 (2006).
9. Forman, R.T.T., Collinge, S.K. Nature conserved in changing landscapes with and without spatial planning. *LANDSCAPE URBAN PLAN*. **37**, 129-135 (1997).
10. Karlson, M., Mörtberg, U., Balfors, B. Road ecology in environmental impact assessment. *ENVIRON IMPACT ASSES*. **48**, 10-19 (2014).
11. Eker, M., Coban, H.O. Impact of road network on the structure of a multifunctional forest landscape unit in southern Turkey. *J ENVIRON BIOL.* **31**, 157-168 (2010).
12. Lin, Y.Y., Hu, X.S., Zheng, X.X., Hou, X.Y., Zhang, Z.X., *et al*. Spatial variations in the relationships between road network and landscape ecological risks in the highest forest coverage region of China. *ECOL INDIC*. **96**, 392-403 (2019).
13. Saunders, S.C., Mislivets, M.R., Chen, J.Q., Cleland, D.T. Effects of roads on landscape structure within nested ecological units of the Northern Great Lakes Region, USA. *BIOL CONSERV*. **103**, 209-225 (2002).
14. Reed, R.A., Johnson-Barnard, J., Baker, W.L. Contribution of roads to forest fragmentation in the Rocky Mountains. *CONSERV BIOL*. **10**, 1098-1106 (1996).
15. Karlson, M., Mörtberg, U. A spatial ecological assessment of fragmentation and disturbance effects of the Swedish road network. *LANDSCAPE URBAN PLAN*. **134**, 53-65 (2015).
16. Eigenbrod, F., Hecnar, S.J., Fahrig, L. Quantifying the road-effect zone: threshold effects of a motorway on anuran populations in Ontario, Canada. *ECOL SOC*. **14**, 1-18 (2009).
17. Wu, C.H.F., Lin, Y.P., Chiang, L.C.H., Huang, T. Assessing highway's impacts on landscape patterns and ecosystem services: A case study in Puli Township, Taiwan. *LANDSCAPE URBAN PLAN*. **128**, 60-71 (2014).
18. Honrado, J.P., Vieira, C., Soares, C., Monteiro, M.B., Marcos, B., *et al*. Can we infer about ecosystem services from EIA and SEA practice? A framework for analysis and examples from Portugal. *ENVIRON IMPACT ASSES*. **40**, 14-24 (2013).
19. Karjalainen, T.P., Marttunen, M., Sarkki, S., Rytkönen, A.M. Integrating ecosystem services into environmental impact assessment: An analytic–deliberative approach. *ENVIRON IMPACT ASSES*. **40**, 54-64 (2013).
20. Xu, H., Wang, M., Shi, T., Guan, H., Fang, C., *et al*. Prediction of ecological effects of potential population and impervious surface increases using a remote sensing based ecological index (RSEI). *ECOL INDIC*. **93**, 730-740 (2018).
21. Xu, H., Wang, Y., Guan, H., Shi, T., Hu, X. Detecting ecological changes with a remote sensing based ecological index (RSEI) produced time series and change vector analysis. *REMOTE SENS-BASEL*. **11**, 2345 (2019).
22. Hu, X.S., Xu, H.Q. A new remote sensing index for assessing the spatial heterogeneity in urban ecological quality: A case from Fuzhou City, China. *ECOL INDIC*. **89**, 11-21 (2018).
23. Reza, M.I.H., Abdullah, S.A. Regional Index of Ecological Integrity: A need for sustainable management of natural resources. *ECOL INDIC*. **11**, 220-229 (2011).
24. Hu, X.S., Xu, H.Q. A new remote sensing index based on the pressure-state-response framework to assess regional ecological change. *ENVIRON SCI POLLUT R*. **26**, 5381-5393 (2019).

25. Kennedy, R.E., Andréfouët, S., Cohen, W.B., Gómez, C., Griffiths, P., *et al*. Bringing an ecological view of change to Landsat-based remote sensing. *FRONT ECOL ENVIRON*. **12**, 339-346 (2014).
26. Dubinin, V., Svoray, T., Dorman, M., Perevolotsky, A. Detecting biodiversity refugia using remotely sensed data. *LANDSCAPE ECOL*. **33**, 1815-1830 (2018).
27. Mishra, N.B., Crews, K.A., Neeti, N., Meyer, T., Young, K.R. MODIS derived vegetation greenness trends in African Savanna: Deconstructing and localizing the role of changing moisture availability, fire regime and anthropogenic impact. *REMOTE SENS ENVIRON*. **169**, 192-204 (2015).
28. White, D.C., Lewis, M.M., Green, G., Gotch, T.B. A generalizable NDVI-based wetland delineation indicator for remote monitoring of groundwater flows in the Australian Great Artesian Basin. *ECOL INDIC*. **60**, 1309-1320 (2016).
29. Healey, S.P., Cohen, W.B., Yang, Z.Q., Krankina, O.N. Comparison of Tasseled Cap-based Landsat data structures for use in forest disturbance detection. *REMOTE SENS ENVIRON*. **97**, 301-310 (2005).
30. Mildrexler, D.J., Zhao, M.S., Running, S.W. Testing a MODIS Global Disturbance Index across North America. *REMOTE SENS ENVIRON*. **113**, 2103-2117 (2009).
31. Rhee, J.Y., Im, J., Carbone, G.J. Monitoring agricultural drought for arid and humid regions using multi-sensor remote sensing data. *REMOTE SENS ENVIRON*. **114**, 2875-2887 (2010).
32. Hu, X.S., Xu, H.Q. Spatial variability of urban climate in response to quantitative trait of land cover based on GWR model. *ENVIRON MONIT ASSESS*. **191**, 194 (2019).
33. Cai, X.J., Wu, Z.F., Cheng, J. Using kernel density estimation to assess the spatial pattern of road density and its impact on landscape fragmentation. *INT J GEOGR INF SCI*. **27**, 222-230 (2013).
34. Hu, X., Zhang, L., Ye, L., Lin, Y., Qiu, R. Locating spatial variation in the association between road network and forest biomass carbon accumulation. *ECOL INDIC*. **73**, 214-223 (2017).
35. Silverman, B.W. Density Estimation for Statistics and Data Analysis, (ed. Chapman and Hall), (New York,1986).
36. Lin, Y., Hu, X., Lin, M., Qiu, R., Lin, J., *et al*. Spatial Paradigms in Road Networks and Their Delimitation of Urban Boundaries Based on KDE. *ISPRS INT J GEO-INF*. 9, 204 (2020).
37. Cohen, W.B., Maiersperger, T.K., Gower, S.T., Turner, D.P. An improved strategy for regression of biophysical variables and Landsat ETM+ data. *REMOTE SENS ENVIRON.* 84, 561-571 (2003).
38. Foody, G.M. Geographical weighting as a further refinement to regression modelling: An example focused on the NDVI–rainfall relationship. *REMOTE SENS ENVIRON*. **88**, 283-293 (2003).
39. Jing, Y.Q., Zhang, F., He, Y.F., Kung, H., Johnson, V.C., *et al*. Assessment of spatial and temporal variation of ecological environment quality in Ebinur Lake Wetland National Nature Reserve, Xinjiang, China. *ECOL INDIC*. 110, 105874 (2020).
40. Fotheringham, A.S., Charlton, M.E., Brunsdon, C. Geographically weighted regression: a natural evolution of the expansion method for spatial data analysis. *ENVIRON PLANN A*. **30**, 1905-1927 (1998).
41. Kupfer, J.A., Farris, C.A. Incorporating spatial non-stationarity of regression coefficients into predictive vegetation models. *LANDSCAPE ECOL*. **22**, 837-852 (2007).
42. You, W., Zang, Z.L., Zhang, L.F., Li, Z.J., Chen, D., et al. Estimating ground-level PM_{10} concentration in northwestern China using geographically weighted regression based on satellite AOD combined with CALIPSO and MODIS fire count. *REMOTE SENS ENVIRON*. **168**, 276-285 (2015).
43. Buyantuyev, A., Wu, J.G. Urban heat islands and landscape heterogeneity: linking spatiotemporal variations in surface temperatures to land-cover and socioeconomic patterns. *LANDSCAPE ECOL*. **25**, 17-33 (2010).
44. Hawbaker, T.J., Radeloff, V.C., Clayton, M.K., Hammer, R.B., Gonzalez-Abraham, C.E. Road development, housing growth, and landscape fragmentation in northern Wisconsin: 1937-1999. *ECOL APPL*. **16**, 1222-1237 (2006).
45. McGarigal, K., Romme, W.H., Crist, M., Roworth, E. Cumulative effects of roads and logging on landscape structure in the San Juan Mountains, Colorado (USA). *LANDSCAPE ECOL*. 16, 327-349 (2001).
46. Tian, L., Chen, J.Q., Yu, S.X. Coupled dynamics of urban landscape pattern and socioeconomic drivers in Shenzhen, China. *LANDSCAPE ECOL*. **29**, 715-727 (2014).

47. Forman, R.T.T., Alexander, L.E. Roads and their major ecological effects. *Annual Review of Ecology and Systematics*. **29**, 207-231 (1998).
48. Yu, W.H., Ai, T.H., Shao, S.W. The analysis and delimitation of Central Business District using network kernel density estimation. *J TRANSP GEOGR*. **45**, 32-47 (2015).
49. Hu, X.S., Zhang, L.Y., Ye, L.M., Lin, Y.H., Qiu, R.Z. Locating spatial variation in the association between road network and forest biomass carbon accumulation. *ECOL INDIC*. **73**, 214-223 (2017).
50. Liu, S.L., Dong, Y.H., Deng, L., Liu, Q., Zhao, H.D., *et al*. Forest fragmentation and landscape connectivity change associated with road network extension and city expansion: A case study in the Lancang River Valley. *ECOL INDIC*. **36**, 160-168 (2014).
51. McGarigal, K., Cushman, S.A., E, E. FRAGSTATS v4: Spatial Pattern Analysis Program for Categorical and Continuous Maps (2012).
52. Xu, H.Q. A remote sensing urban ecological index and its application. *Acta Ecologica Sinica*. **33**, 7853-7862 (2012).
53. Fotheringham, A.S., Brunsdon, C., Charlton, M. Geographically Weighted Regression: The Analysis of Spatially Varying Relationships, (ed. Wiley), (Chichester, 2002).
54. Xu, H.Q. Modification of normalised difference water index (NDWI) to enhance open water features in remotely sensed imagery. *INT J REMOTE SENS*. **27**, 3025-3033 (2006).

Tables

Table 1
Tests of the ordinary least squares (OLS) and the geographically weighted regression (GWR) models.

Dependent variables	Independent variable	GWR					OLS		
		Adjusted R-squared	AICc	Residual Squares	P-value	Moran's I	Adjusted R-squared	AICc	P-value
NDVI	KDR	0.492	-1593.980	364.288	0.001	0.264	0.042	3301.775	0.05
IBI		0.316	-11106.919	107.524	0.001	0.246	0.069	-8745.447	0.05
SI		0.555	-17968.641	44.592	0.001	0.218	0.113	-12639.017	0.05
NDBSI		0.433	-18944.724	39.344	0.001	0.199	0.160	-15917.960	0.05
LST		0.483	41251.776	88770.466	0.001	0.309	0.168	44910.860	0.05
LSM		0.314	-23242.687	22.670	0.001	0.250	0.013	-20447.086	0.05
RSEI		0.564	-16837.017	51.558	0.001	0.213	0.138	-11557.232	0.05

Table 2

Coefficient statistics of the geographically weighted regression (GWR) models.

Dependent variables	Independent variable	Parameter descriptive statistics				
		Minimum	Average	Median	Maximum	Standard deviation
NDVI	KDR	-1.261	-0.133	-0.084	0.530	0.214
IBI		-0.219	0.040	0.033	0.348	0.072
SI		-0.130	0.071	0.039	0.681	0.098
NDBSI		-0.063	0.055	0.032	0.501	0.071
LST		-7.145	1.958	1.604	15.238	2.635
LSM		-0.124	-0.010	-0.008	0.121	0.032
RSEI		-0.706	-0.080	-0.046	0.123	0.103

Table 3. Pearson correlation analysis (** indicates statistically significant at 0.01 level).

Indicators	IBI	LST	NDBSI	NDVI	SI	LSM	RSEI	Color chart	R^2
IBI	1	0.957**	0.776**	-0.060**	0.397**	-0.918**	-0.428**		0.85~0.99
LST	0.912**	1	0.786**	-0.123**	0.444**	-0.901**	-0.482**		0.70~0.84
NDBSI	0.800**	0.807**	1	-0.674**	0.887**	-0.535**	-0.900**		0.50~0.69
NDVI	0.414**	0.264**	-0.208**	1	-0.937**	-0.232**	0.926**		-0.49~0.49
SI	0.084**	0.205**	0.665**	-0.860**	1	-0.107**	-0.997**		-0.69~-0.50
LSM	-0.935**	-0.865**	-0.673**	-0.523**	0.047**	1	0.148**		-0.84~-0.70
RSEI	-0.136**	-0.275**	-0.697**	0.840**	-0.989**	0.011	1		-0.99~-0.85

Figures

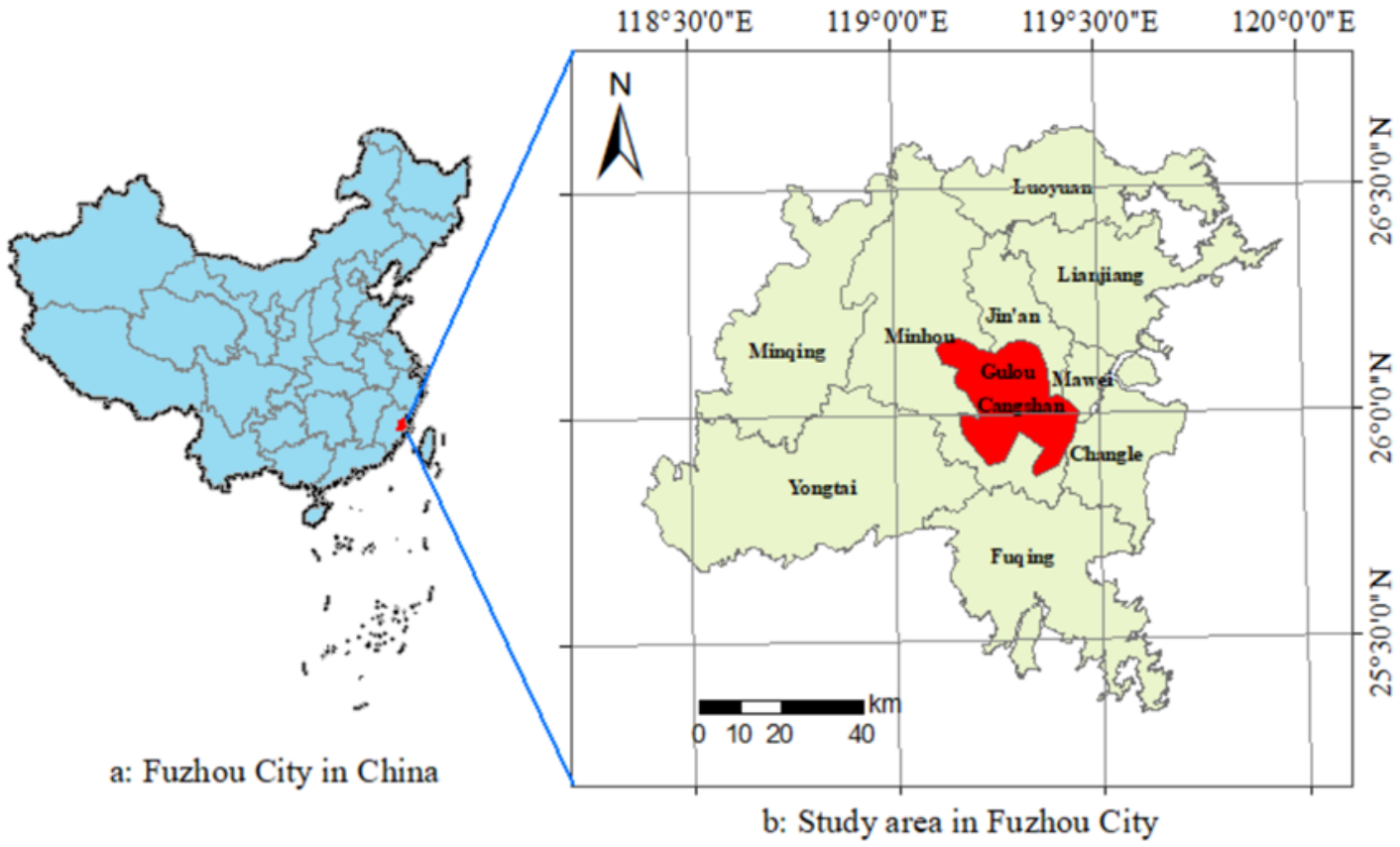

Figure 1

Location of the study area

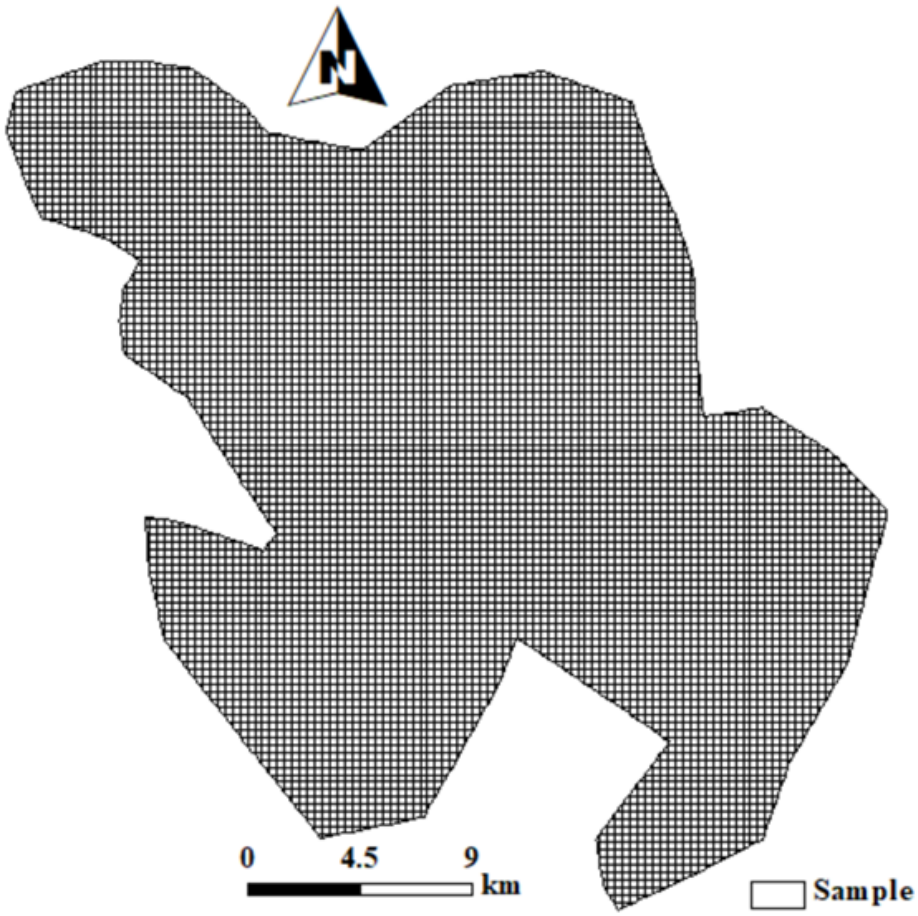

Figure 2

Samples (300×300 m)

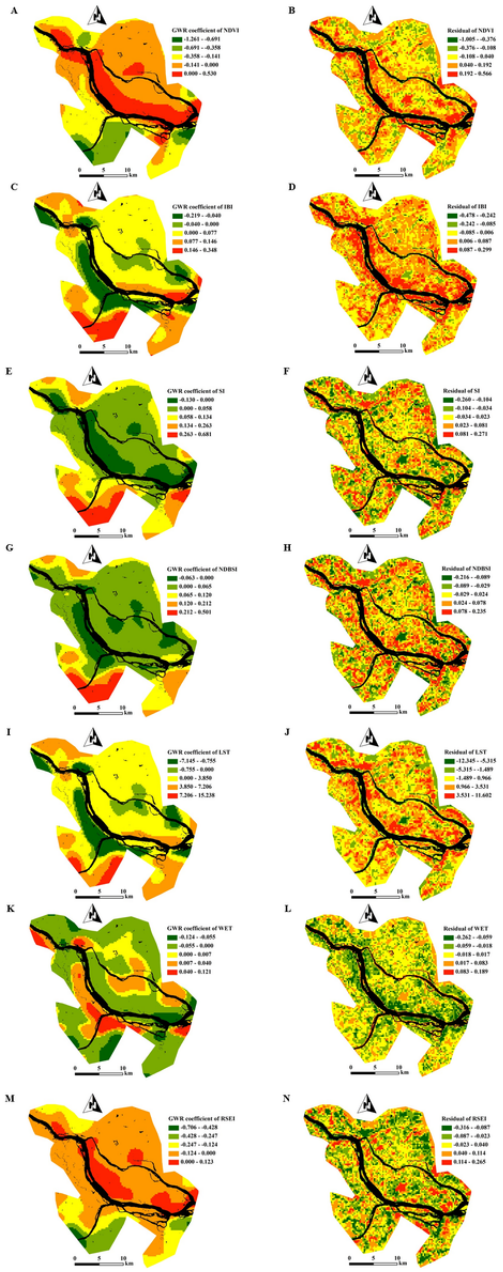

Figure 3

Geographically weighted regression (GWR) coefficient and residual of different eco-environmental indicators against kernel density of road (KDR). (A,B) normalized difference vegetation index (NDVI) against KDR; (C,D) index-based built-up index (IBI) against KDR; (E,F) soil index (SI) against KDR; (G,H) normalized differential build-up and bare soil index (NDBSI) against KDR; (I,J) land surface temperature (LST) against KDR; (K,L) land surface moisture (LSM) against KDR; (M,N) remote sensing based ecological index (RSEI) against KDR.

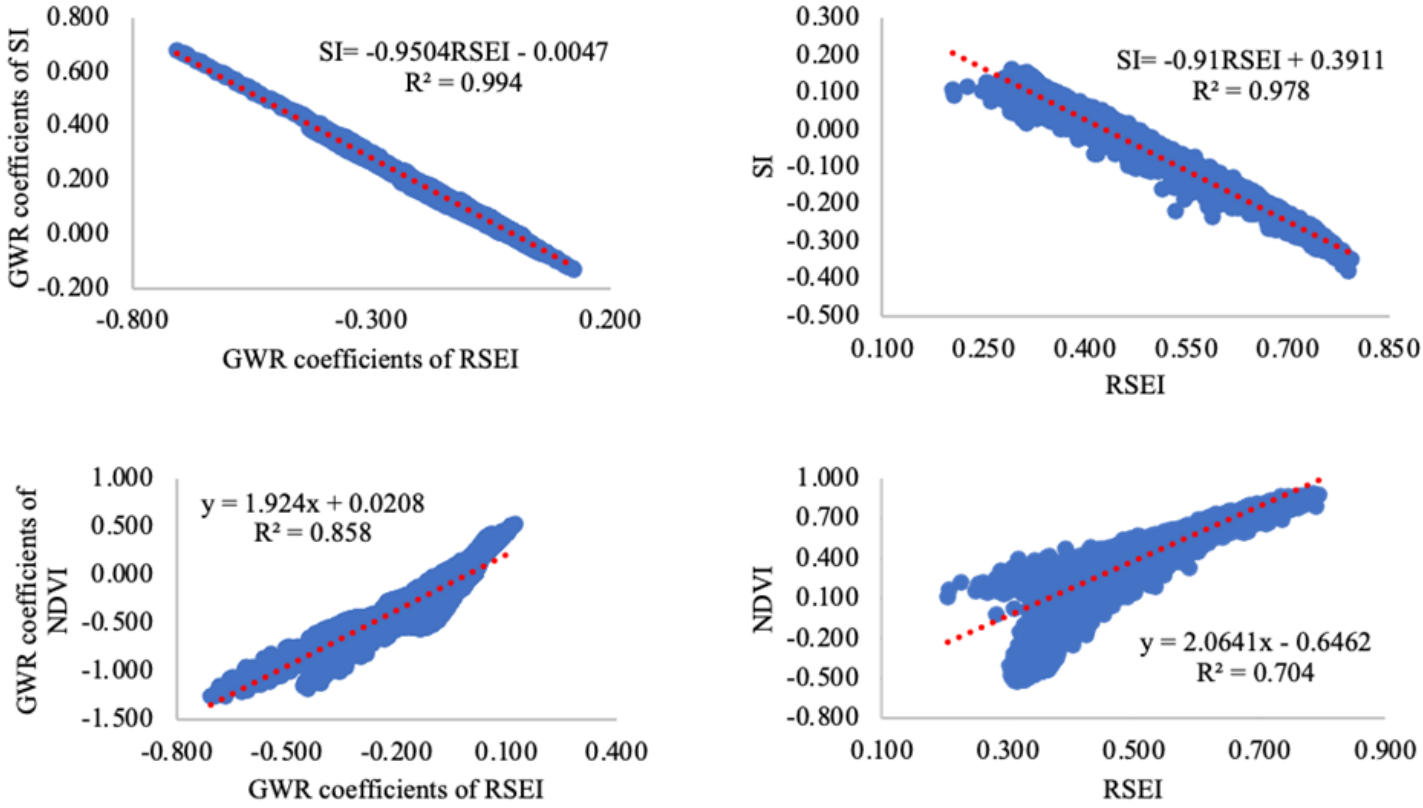

Figure 4

Scatter plots of coefficients of remote sensing based ecological index (RSEI), soil index (SI) and normalized difference vegetation index (NDVI).